

## Relaxation and fluctuation effects near the melting transition in a two-dimensional solid

Anthony D. Novaco and Philip A. Shea

*Department of Physics, Lafayette College, Easton, Pennsylvania 18042*

(Received 24 February 1982)

A molecular-dynamics simulation was used to examine the approach to equilibrium of a two-dimensional solid near the melting transition. The system examined consisted of 256 particles interacting through an  $r^{-5}$  repulsive potential. It was found that near the transition the behavior is characterized by both increasing relaxation times and increasing thermodynamic fluctuations. No true metastable states were observed. This behavior appears to be the critical slowing down that accompanies continuous transitions, supporting the view that melting in two dimensions, at least under some circumstances, is continuous. Estimates of the effects of those fluctuations which are suppressed because of the finite size of the system further supports this view. The transition temperature was found to be consistent with the Kosterlitz-Thouless dislocation hypothesis for melting but the system was too small to make any reliable statements about the existence of the hexatic phase proposed by Nelson and Halperin.

### I. INTRODUCTION

The nature of melting in two-dimensional systems has been studied for many years, and yet this phenomenon is still the subject of much controversy.<sup>1-3</sup> The great interest which has developed over the last few years in this subject has been generated, to a large extent, by some recently proposed theoretical models for this transition. The theory of Kosterlitz and Thouless predicts a second-order melting process driven by the unbinding of dislocation pairs.<sup>4</sup> A later enhancement of this theory derived by Nelson and Halperin predicts that melting should occur in two stages, the first stage producing a proposed anisotropic liquid phase (the hexatic phase) and the second stage (at higher temperature) resulting in the normal isotropic liquid.<sup>5-7</sup> The lower-temperature transition is predicted to be the Kosterlitz-Thouless transition for which the Lamé coefficients  $\lambda$  and  $\mu$  of the solid just below melting are related to the transition temperature  $T_c$  by

$$4\pi kT_c = \frac{\mu(\lambda + \mu)}{\lambda + 2\mu} a_0^2, \quad (1)$$

where  $a_0$  is the lattice constant and  $k$  is the Boltzmann constant. The solid is predicted to have algebraic decay of translational order but long-range orientational order. The hexatic phase should have algebraic decay of orientational order and exponential decay of translational order. The

isotropic liquid has, of course, exponential decay of both.

Throughout the history of the study of melting, both in two- and three-dimensional systems, computer simulations have played an important role. Early simulations of hard-disk systems and those with  $r^{-n}$  repulsive interactions indicated that melting in two dimensions is not very different than that in three. In particular, early studies indicated that the transition was first order as evidenced by the existence of a two-phase region.<sup>8</sup> Later simulations of Lennard-Jones systems showed a similar behavior.<sup>9</sup> In fact, the co-existence between solid and liquid phases with the concomitant metastable states and hysteresis remains the main argument of those that claim a first-order transition for two-dimensional melting. Unfortunately, an apparent two-phase region can also be caused by finite-time and finite-size effects in the model system. It is these effects, in particular the finite-time effects, that we examine in this paper.

Recent work has cast serious doubt upon the conclusions of some of the earlier studies, attributing the apparent first-order behavior to the lack of equilibrium in the system. Frenkel and McTague gave the first simulation evidence that the melting transition might be a continuous transition driven by the Kosterlitz-Thouless and Nelson-Halperin mechanisms.<sup>10</sup> These conclusions have not gone unchallenged, however, and new evidence has been presented on both sides of the question.<sup>11-17</sup> Al-

though the data reported in these studies is very similar, the conclusions reached are often very different.

In previous studies, the reported results indicated that often only passing thought is given to the question of whether or not the system is in equilibrium. At best, the system is run for a "long" time before "long" time averages are calculated without any quantitative justification of whether "long" is indeed long enough. At worst, little consideration is given to this question. What has been lacking is a detailed study of the approach to equilibrium and some *quantitative* criterion used to determine if a given average is reliable or not. We show that a simple quantitative criterion can be used to determine which averages are valid (equilibrium) averages and then use this criterion to examine the fluctuations near the melting transition. These fluctuations make the evaluations of time averages near the transition very difficult if not impossible. Under these circumstances, improper averaging can and does produce the type of hysteresis usually associated with a first-order transition. However, if care is taken to examine the time dependence of this hysteresis, much of the evidence for a first-order transition disappears. We used this criterion to examine the time behavior of each constant-energy run. If only those averages which are judged by this criterion to be valid are accepted, the hysteresis is greatly reduced, and the transition looks very much like a continuous transition. In the end, we conclude that no valid conclusions about melting in two dimensions can be drawn from any molecular-dynamics calculation without doing a very careful quantitative study of the relaxation effects near melting. It is *not* sufficient to run for some arbitrarily long period of time before starting the calculation of the time average and then average over what appears to be a long time based upon some qualitative criterion or "rule of thumb." This is because relaxation times very near the transition appear to be much longer than any conceivable molecular-dynamics run.

## II. RELAXATION EFFECTS NEAR MELTING

We have examined a system of particles interacting with an  $r^{-n}$  repulsive interaction with  $n = 5$ . There was no particular reason for choosing 5, except that it is a "reasonable" choice between the "hard" Lennard-Jones repulsion value ( $n = 12$ ) and the "very soft" Coulomb gas value ( $n = 1$ ). It is

expected that the softer potentials are more likely to exhibit Kosterlitz-Thouless melting.<sup>18</sup> The advantages of inverse  $r$  potentials are well known, namely, producing a phase diagram not complicated by the existence of a liquid-gas transition and possessing special scaling rules which allow the generation of an entire phase diagram from a single isochore.<sup>19</sup> This latter property is very useful in molecular-dynamics studies since the "natural" path for the dynamics is that of an isochore while the most useful path for studying the nature of a given transition is an isobar or an isotherm. Naturally, this scaling holds only for *equilibrium* data.

If we write the interaction potential as

$$v(r) = \epsilon \frac{\sigma^n}{r^n}, \quad (2)$$

then  $\eta = (\rho\sigma^2)(\epsilon/kT)^{2/n}$  is the important thermodynamic variable and all thermodynamic functions scale along lines of constant  $\eta$ . The natural (reduced) units for this system are  $\epsilon$  for energy,  $\sigma$  for distance, and  $\tau = (m\sigma^2/\epsilon)^{1/2}$  for time, where  $m$  is the mass of the particle. These units are used for all quantities reported in this work.

Since it was recognized that relaxation effects would likely be very important, precautions were taken to ensure that the system was initialized, heated, and cooled as gently as possible. Except for these precautions, the actual mechanics of the molecular-dynamics procedure was quite standard.<sup>20</sup> The initialization, heating, and cooling procedures are discussed in the Appendix. All runs were along a single isochore with a density of  $1/\pi$ , and all results are reported for a system of 256 particles. Constant energy runs were divided into blocks of 1000 steps and the time averages for thermodynamic variables over each block were written to a disk file for later analysis. This was done a maximum of 99 times for any run, so that the longest run was 99 000 time steps. Near the transition, it was absolutely necessary to run all simulations for this period of time and even then much data still showed strong relaxation effects and could not be included in the equilibrium averages.

It was found that the best way to judge if the system has come to equilibrium is to examine the time dependence of the autocorrelation functions of various thermodynamics quantities. These functions enabled us to determine if the system had run long enough to "forget" its initial configuration before averages were calculated. Furthermore, these

functions established a *quantitative* criterion for determining the minimum time period required for a valid average. Decisions were based upon graphical estimates for the relaxation times of the autocorrelation functions. As a general rule, averages were not calculated until the system had been run at constant energy for about one relaxation time and averages were then calculated over several relaxation times. It was found that these restrictions ensured that averages from independent runs (runs generated from independent initializations) were reproducible and did not depend upon prior heating or cooling. Runs which did not satisfy these restrictions were found to exhibit hysteresis, that is, the averages depended upon the history of the runs and independent runs did not exhibit reproducible results. It was also found that the relaxation associated with a given run is independent of which thermodynamic variable is used to define the relaxation time. This is true even for variables which are as different as the temperature and the orientational order parameter  $\psi_6$  where we have defined this to be

$$\psi_6 = \frac{\sum_{ij} \exp(i6\theta_{ij})}{\sum_{ij} 1} \quad (3)$$

The sums over  $i$  and  $j$  include only those pairs with a separation less than  $r_0 = 1.44$ . This radius is essentially the distance at which the pair-distribution function reaches its minimum value between the first- and second-nearest-neighbor peaks.

Instead of evaluating the autocorrelation functions for the step-by-step values of the thermodynamic variables, it is sufficient, for our purposes here, to evaluate these functions for the block averages discussed above. If  $\{T_i\}$  represents, for example, the set of temperature block averages for a given constant energy run, then the appropriate autocorrelation function is given by

$$\langle\langle T_i; T_0 \rangle\rangle = \frac{\langle T_{i+n} T_n \rangle_n - \langle T_n \rangle_n^2}{\langle T_n T_n \rangle_n - \langle T_n \rangle_n^2} \quad (4)$$

where  $\langle \rangle_n$  refers to the average over  $n$ . In general, the maximum value of  $i$  was chosen to be  $\frac{1}{4}$  of the maximum number of block averages for a given run and the sum over  $n$  was carried out for evenly spaced values of  $n$  between zero and the total number of block averages for the run *minus* the maximum value of  $i$ . Usually, 25 values of  $n$  were sufficient to produce reliable results.

Figure 1 shows the temperature  $T$ , calculated

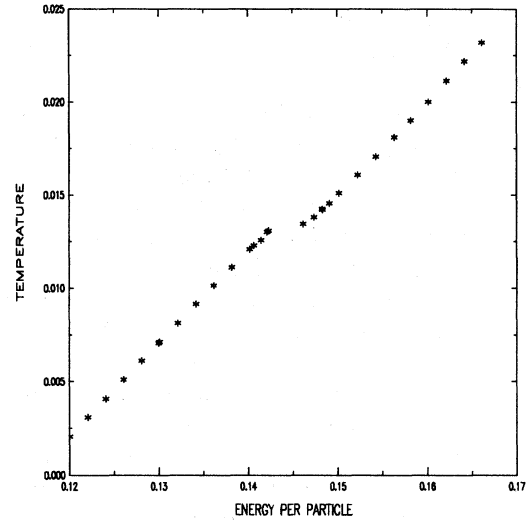


FIG. 1. Average temperature calculated using the equipartition theorem. The gap in the data for energies between 0.142 and 0.146 shows the extent of the transition region. All data shown are equilibrium data.

from the equipartition theorem, as a function of the energy  $E$ . Only those runs satisfying the above acceptance criterion are shown. There is a distinct gap in the data for energies between 0.142 and 0.147. All runs in this energy range showed relaxation effects on a very-long-time scale. This gap delimits the transition region, defining this region as that range of energies bounded by points at which the relaxation times increased or decreased sharply. Such points are quite easy to locate. If the block averages are truly independent (no relaxation effects) then the autocorrelation functions should look like that in Fig. 2(a), the autocorrelation function of a set of 100 random numbers. Note that this function is not zero for  $i > 0$  because of finite sample effects. Figures 2(b) and 2(c) show temperature autocorrelation functions for runs which are somewhat above and somewhat below the transition region. The similarities between these two figures and Fig. 2(a) show that any relaxation effects in these runs decay within 1000 time steps. Time averaging starting with the second block average and including several blocks produces reliable equilibrium averages.

Figures 3(a)–3(c) show what happens to the autocorrelation functions at the boundaries of and within the transition region. Note the lengthening of the relaxation time. Figure 3(b), which corresponds to the system placed in the middle of the transition region, shows that the relaxation time is much longer than the time interval shown. Since this time interval corresponds to 25 000 time steps

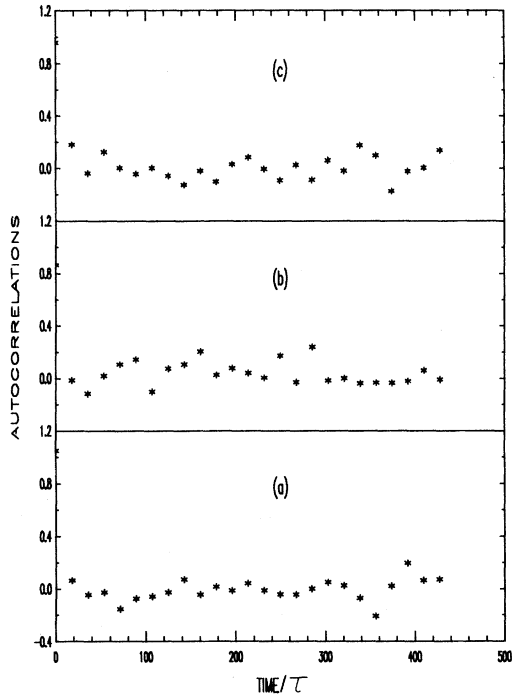


FIG. 2. Comparison of three autocorrelation functions showing a lack of any relaxation effects: (a) autocorrelation function for 100 random numbers, (b) autocorrelation function for run at energy of 0.1402, and (c) run at energy of 0.1523. Run (b) is in the solid phase and (c) is in the liquid phase.

and the run was continued for nearly 100 000 time steps, any average based upon this run would be suspect and unreliable. In fact, it appears that runs in excess of 500 000 time steps would be the minimum needed before reliable averages could be obtained. These figures also demonstrate that relaxation effects for the temperature and for  $\psi_6$  are essentially the same. Similar effects were observed for other thermodynamic functions. These relaxation effects are accompanied by a dramatic increase in the amplitude of the fluctuations. Figure 4 shows

$$\frac{\langle T_n T_n \rangle_n - \langle T_n \rangle_n^2}{\langle T_n \rangle_n^2}, \quad (5)$$

the relative variance of the temperature block averages, as a function of the energy. The large peak in this relative variance reflects a corresponding increase in the fluctuations of the step-by-step temperatures. This increase in the fluctuation amplitude correlates quite well with the increase in the relaxation time. Thus as the transition is approached from either side, there is a marked change in the thermodynamic fluctuations which

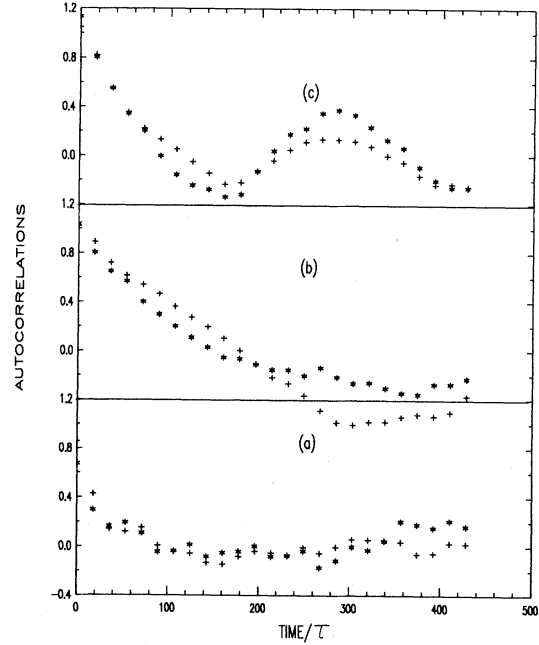


FIG. 3. Comparison of three autocorrelation functions showing relaxation effects: (a) autocorrelation function for run at energy of 0.1415, (b) at 0.1449, and (c) at 0.1462. Run (a) is at the solid boundary of the transition region, run (c) is at the liquid boundary, and (b) is in the middle. The \*'s show the temperature autocorrelations while the +'s show the  $\psi_6$  autocorrelations.

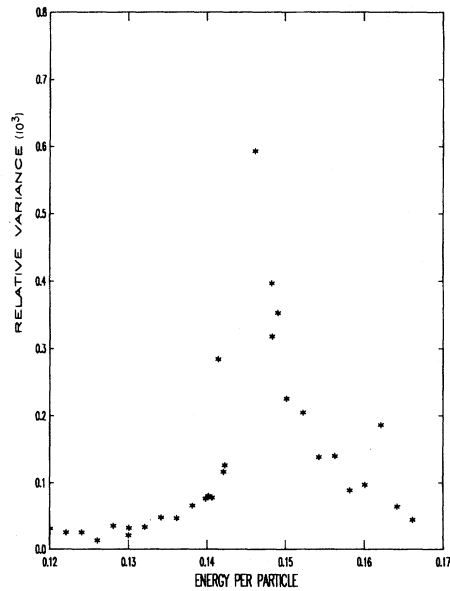


FIG. 4. Relative variances of the temperature-block averages. Note the dramatic increase in the amplitude of the temperature fluctuations as the transition is approached from either higher or lower energies.

simultaneously increase in amplitude and slow down.

### III. THERMODYNAMIC RESULTS

In the standard molecular-dynamics run, the energy, area, and particle number are fixed. However, the best way to examine the nature of a transition is to display the data as an isobar or isotherm. If temperature (isobar) or pressure (isotherm) is plotted as a function of the area (or density), then any two-phase region will be characterized by a horizontal line whose endpoints define the boundaries of the two-phase region. Of course, in a finite system this horizontal line will not actually be observed.<sup>21</sup> Nevertheless, there should appear two branches in each plot, with two definable points which represent the endpoints of the two-phase region. The endpoint pairs in each plot must have the same pair of values for  $\eta$ . Furthermore, there should be no relaxation associated with either endpoint since these represent a single-phase system. It would also be expected that metastable states corresponding to supercooling and superheating should be observable. These metastable states should be characterized by long-time behavior showing nucleation effects rather than relaxation effects.<sup>22</sup> Figures 5 and 6 show isobar and isotherm plots generated from the isochore data through use of the scaling equations for the inverse

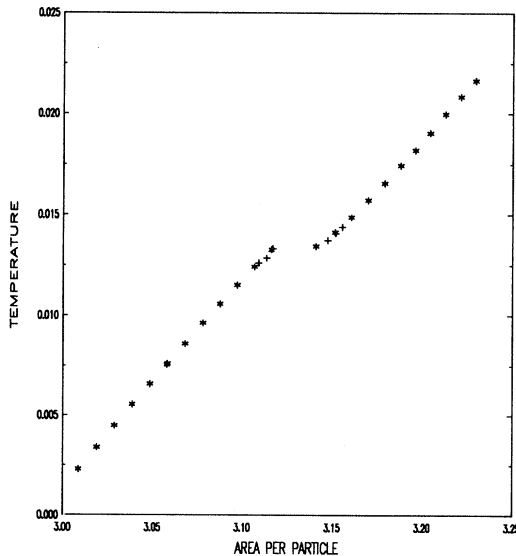


FIG. 5. Isobar generated from the data shown in Fig. 1 by using the scaling equations. Runs generated by heating are plotted with \* and those generated by cooling are plotted with +.

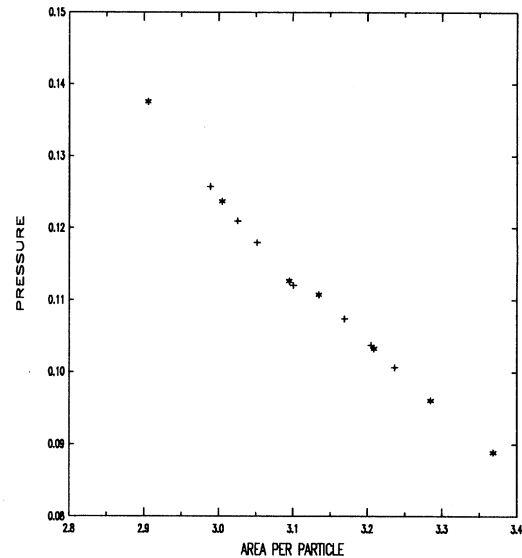


FIG. 6. Isotherm generated from the data shown in Fig. 1 by using the scaling equations. Runs generated by heating are plotted with \* and those generated by cooling are plotted with +.

$r$  potentials.<sup>19</sup> The pressure  $P$  and temperature  $T$  are plotted as a function of the area  $A$ . Note that each plot there is a noticeable gap in the data for a range of areas between 3.115 and 3.142. This gap corresponds to the gap in Fig. 1 with the data inside this gap showing strong relaxation effects, having relaxation times so long that reliable averages could not be calculated *even* for runs of 100 000 time steps. However, outside of this range the data is reproducible and independent of whether it was obtained from a set of runs generated through cooling or a set of runs generated by heating. In both the isobar and the isotherm plots, relaxation effects become important before the branches can reach a common temperature (isobar) or pressure (isotherm). This is most noticeable in the isotherm plot, but also can be seen clearly in the isobar plot if the scale of the plot is enlarged. This is done in Fig. 7 which also includes averages which are not equilibrium averages, based upon the criterion in the preceding section. Nevertheless, these averages were for entire runs of 99 000 time steps and are typical of the sort of results reported in many papers. Note that there is indeed hysteresis in the data. However, this hysteresis is time dependent with the amount of hysteresis decreasing *very slowly* as the length of the run is increased. The fact that it is indeed relaxation and *not* metastability is shown clearly by the autocorrelation functions but is very difficult to see by simply plotting the thermodynamic functions versus time.

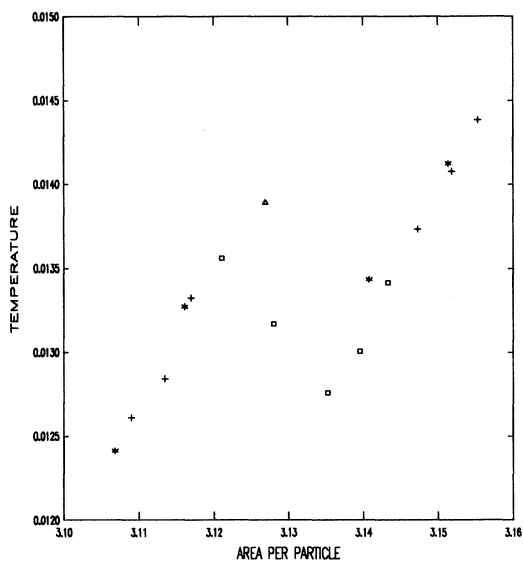


FIG. 7. Isobar using an expanded scale for the area and including very-long-time averages which did not satisfy the acceptance criterion of Sec. II. Equilibrium values are given by \* for runs generated by heating and + for those generated by cooling. Nonequilibrium long time averages are given by  $\Delta$  for the heating cycle and by  $\square$  for the cooling cycle.

If such plots are drawn, they show *no* evidence of nucleation of the sort seen for three-dimensional systems.<sup>22</sup> Rather, they show fluctuations with large amplitudes and very long periods. Again, the autocorrelation functions, which show a damped oscillator behavior, are the clearest evidence for these relaxation effects. Figure 7 also shows that once beyond the region of strong relaxation effects, the runs obtained by cooling resulted in the same averages as those obtained by heating. However, it is very important to allow each cooling cycle to take place only after the system has run at constant energy for a *long* time, preferably about one relaxation time. Heating the system was not as delicate a process, but it also is preferable to run the system at constant energy for some period of time between heating cycles.

Both Figs. 5 and 7 show that on the liquid side of the transition region, there is noticeable rounding of the isobar. Furthermore, the fluctuations in thermodynamic functions such as the temperature increased dramatically as the transition region was approached from either end as shown in Fig. 4. These fluctuations can also be seen in the step-by-step temperatures and give rise to a peak in the specific heat. Using the step-by-step averages of the square of the temperature it is possible to calculate the specific heat at constant area,<sup>23</sup> but it is

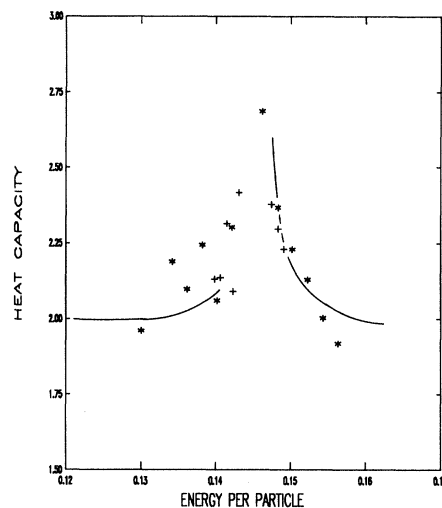


FIG. 8. Specific heat at constant area as a function of the energy per particle. The points show the results of a calculation of the specific heat using temperature fluctuations while the solid lines are smooth curves drawn through points calculated by differentiating the data in Fig. 1 as explained in the text.

necessary to average  $T^2$  over very long runs in order to obtain reasonable values. Thus the data shown in Fig. 8 are only for the longest runs made. The curves drawn in that figure represent values obtained by an approximate differentiation of the temperature versus energy data in Fig. 1. A simple point-by-point first-difference scheme was used to obtain the derivative, and a smooth line was drawn through the calculated points. The uncertainty in the calculated values using the differentiation scheme is between 1% and 3%, being less further from the transition. The agreement between this scheme and the fluctuation calculation is reasonably good.

In Fig. 9 we show  $|\psi_6|$  as a function of the energy. This graph shows runs obtained by both heating and cooling and includes both equilibrium data and nonequilibrium data. Each class of data is represented separately. The sudden decrease in  $|\psi_6|$  occurs at the solid boundary of the transition region. The slight amount of hysteresis is associated entirely with the nonequilibrium runs, which are the same runs shown in Fig. 7. The equilibrium runs show a set of consistent values for  $|\psi_6|$  independent of whether the run was generated from a heating or a cooling cycle. Because of the long relaxation times in the transition region, it is not possible to describe the precise behavior of  $|\psi_6|$  at the transition. However, it is clear that the order parameter decreases very quickly, in a very narrow temperature range, from a value of about 0.66 to

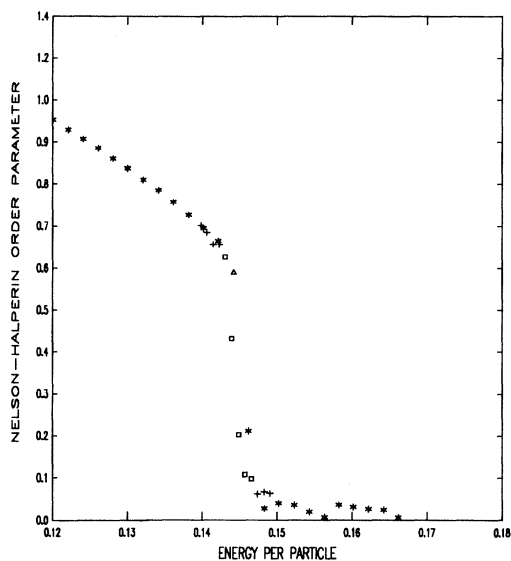


FIG. 9. Absolute value of the Nelson-Halperin order parameter as a function of the energy per particle showing both equilibrium and nonequilibrium data. Equilibrium data for the heating cycle are given by \* while + gives the equilibrium data for the cooling cycle. The nonequilibrium long-time averages are given by  $\Delta$  for heating and by  $\square$  for cooling.

zero as melting is reached. Above the transition, the standard deviation of the order parameter is larger than the average value, indicating that it is statistically zero as expected. It was impossible to come to any defensible judgments about finite-size effects upon  $|\psi_6|$  or upon the existence of the hexatic phase.

While the order parameter is decreasing very rapidly as the transition is reached, the self-diffusion constant  $D_s$  is *increasing* very rapidly, as shown in Fig. 10. In this graph, the values of  $|\psi_6|$  and  $D_s$  were calculated over the same set of 10000 step runs and the equilibrium criterion was not applied to these averages. The diffusion constant was calculated from the asymptotic slope of the average of the square of the relative displacement at "large" times.<sup>24</sup> These values were checked against values obtained by the integration of the velocity autocorrelation function and the two methods were found to agree to within about 10%. The complementary behavior of  $D_s$  and  $|\psi_6|$  is rather obvious from the graph. Where no value of  $D_s$  is shown corresponding to a given value of  $|\psi_6|$ , then that diffusion constant was found to be zero.

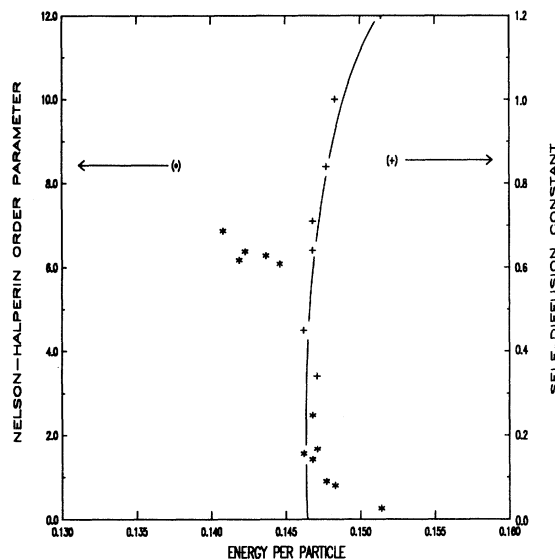


FIG. 10. Comparison of the Nelson-Halperin order parameter (\*) and the self-diffusion constant (+), both calculated for the same set of 10000 step runs. If a value for the order parameter is shown without a corresponding value for the diffusion constant, that diffusion constant was found to be zero. The curve drawn through the diffusion constant data is drawn *only* as an aid for the eye.

#### IV. CONCLUSIONS

It is always dangerous to draw unqualified conclusions about the nature of any phase transition from the results of a simulation without a careful study of both the finite-time effects and the finite-size effects inherent in any such calculation. Nevertheless, an examination of the results of the last section gives more support to the view that melting in two dimensions is a continuous transition and presents some serious problems for the view that it is first order. Perhaps the most significant evidence in favor of the view that it is continuous is the fact that in both the isotherm and isobar plots it was not possible to find a common pressure (isotherm) or temperature (isobar) for both branches due to the onset of relaxation effects. The fact that the relaxation effects are accompanied by increases in the corresponding fluctuation amplitudes indicates that the phenomena observed is the critical slowing down which accompanies continuous transitions.<sup>25</sup> Furthermore, the decrease in the order parameter  $|\psi_6|$  and the increase in the specific heat are characteristic of such transitions. No metastable states, in the usual

sense of the term, were observed.<sup>22</sup> Thus the two most characteristic phenomena associated with a first-order transition were not found in this system. Finite-size effects<sup>21</sup> would not be expected to account for this negative result since the finite system tends to stabilize not destabilize the metastable states.

A check of the Kosterlitz-Thouless idea of dislocation unbinding can be made by comparing  $T_c$  calculated from Eq. (1) to what is actually observed in the simulation. What is needed for this comparison is an evaluation of the Lamé coefficients just below melting. This evaluation was carried out via two techniques. The first technique was the standard analysis of the transverse currents to calculate the second-order elastic coefficients and from these the Lamé coefficients.<sup>26</sup> The fluctuations in the transverse currents were averaged over runs of 10 000 steps using samples of 100 to 200 configurations. This calculation produced elastic coefficients which were accurate to about 15–20% as judged by the degree to which the isotropy condition and the density-current sum rule were satisfied.<sup>26</sup> An independent check of the Lamé coefficients obtained in this manner was made by an analysis of the dynamic structure factor  $S(\vec{Q}, \omega)$ . First, the autocorrelation function  $S(\vec{Q}, t)$ , where

$$\begin{aligned} S(\vec{Q}, t) &= \langle \langle f(\vec{Q}, t); f(\vec{Q}, 0) \rangle \rangle, \\ f(\vec{Q}, t) &= \sum_j \exp[i\vec{Q} \cdot \vec{r}_j(t)], \end{aligned} \quad (6)$$

were calculated from step-by-step configurations in a 10 000 step run. Then  $S(\vec{Q}, \omega)$ , the temporal Fourier transform, was calculated and examined for peaks which would signal the existence of propagating modes in the solid. Figure 11 shows a typical plot of  $S(\vec{Q}, \omega)$  for a run just below the melting transition. There are spurious oscillations in this plot due to the finite-step and finite-range limitations of the integration over time. Nevertheless, the peak in  $S(\vec{Q}, \omega)$  is quite distinct. By choosing the relative orientation of  $\vec{Q}$ , the scattering vector, and  $\vec{q}$ , the wave vector of the propagating mode, it is possible to separate the contributions of the longitudinal and the transverse modes.<sup>27</sup> This analysis only requires that the two modes be uncoupled and this is always the case for  $\vec{q}$  along a high-symmetry direction. Vibrational frequencies were calculated at various points in the first and second Brillouin zones to ensure that these frequencies had the periodic behavior expect-

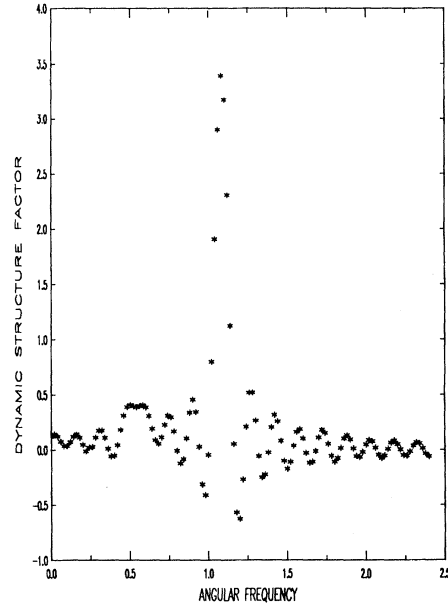


FIG. 11. Dynamic structure factor  $S(\vec{Q}, \omega)$  for a typical case just below the melting transition. The rapid oscillations are caused by finite-time-step and finite-range limitations in the integration of  $S(\vec{Q}, t)\exp(i\omega t)$ .

ed of such modes. A plot of  $\omega$  vs  $\vec{q}$  along a high-symmetry direction is shown in Fig. 12 for both modes. These frequencies were obtained in the vicinity of the (1,0) “Bragg” peak. By estimating both sound velocities from these graphs and using standard continuum theory,<sup>28</sup> it is possible to obtain the Lamé coefficients. These values are  $\lambda=0.31$  and  $\mu=0.05$ , which are to be compared to the values of 0.32 and 0.05 found by the transverse-current method. The  $S(\vec{Q}, \omega)$  method appears to be less susceptible to variations than is the case with the transverse-current method. Using Eq. (1), we then obtain a value for  $T_c$  of about 0.013, while the simulation shows the transition to occur between 0.013 and 0.014. This agreement is striking. It should be noted that although we did not examine the free energy of the system, we would expect that our transition temperature is the thermodynamic transition and not the upper limit to the stability of the solid.<sup>16</sup> We base this judgment upon our analysis of the isotherms and the fact that this data should reflect equilibrium states. If metastable states had indeed been observed, this presumption would not be justified and it would then be necessary to perform a free-energy analysis to determine the thermodynamic transition.

While the evidence for a continuous melting transition is strong, the evidence for an hexatic intermediate phase is not. Because of the small size

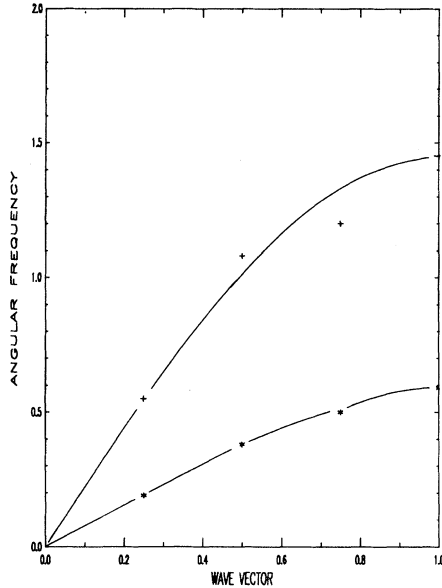


FIG. 12. Longitudinal and transverse frequencies for density waves in the solid along the line from the center of the hexagonal Brillouin zone to the midpoint of one of the sides. The curves shown are the qualitative best fit. The slope of each curve, in the limit of small  $\vec{q}$ , gives the corresponding sound velocity and these are used to calculate the Lamé coefficients.

of our system, we did not examine the behavior of the  $\psi_6$  correlation function. Such an analysis is the best way to detect the existence of this phase.<sup>10</sup>

We did, however, examine the dependence of the static structure factor  $S(\vec{Q})$  upon both the magnitude and direction of  $\vec{Q}$ . Below the melting transition,  $S(\vec{Q})$  showed the expected Bragg peaks for a simple hexagonal lattice. We found the width of these peaks to be dominated entirely by the finite size of the system. The peak width is identical to that of 256 particles arranged in a  $16 \times 16$  hexagonal array. As the transition is approached from below, the width remains constant and the height steadily decreases. The decrease in the height of the peak is associated with the thermal motion of the particles about their lattice sites. The constant width indicates that the correlation length associated with any disordering phenomena (like pairs of dislocations) was much larger than the size of the system. Any increase in the width of the peaks due to these dislocations would have to be in the region where strong relaxation effects were found. A calculation of the population of dislocation pairs in the spirit of Ref. 17 showed that this population was less than 5% of the number of particles for those runs that were in equilibrium. It is clear that much longer runs with larger systems will be

necessary if the effects of the dislocations upon the width of the structure factor are to be reliably calculated.

Above the transition,  $S(\vec{Q})$  showed the expected lack of any "long-range" order. However, it did appear that the structure factor was not isotropic as expected. It is not clear if the observed anisotropic behavior is evidence for an anisotropic fluid or has some other less exotic explanation. Much longer runs on a larger system and a careful consideration of any effects of the boundary would be necessary before any conclusions could be drawn.

Up to this point, we have said little about any finite-size effects for this system. While a careful determination of the size dependence of various thermodynamic and structural quantities is a sizable task (given the very long runs that are necessary in the transition region), there is one interesting consideration which does have an important bearing on any examination of the melting transition. If the transition were first order, then self-consistency suggests that density fluctuations in the solid phase just below the melting temperature must be small enough so that no significant portion of the solid is likely to be found at a density equal to that of the liquid. If this is not the case, then it would be reasonable to expect that the interface between the solid and liquid phases in the two-phase region would be unstable. It is then of some value to examine the density fluctuations associated with large wavelengths and to compare the size of these fluctuations to the difference between the solid and liquid phases interpreting the gap in Fig. 1 as a two-phase region instead of a critical region. Density fluctuations associated with regions larger than the size of our system can be calculated by using the Lamé coefficients calculated for the finite system as good estimates of the Lamé coefficients of the macroscopic system. Calculating the rms fluctuations in the density  $\rho$  due to the longitudinal modes we find

$$\langle (\delta\rho)^2 \rangle_{\text{rms}} = \frac{4T\rho}{\Omega} \sum_{\vec{q}} \frac{(\vec{q} \cdot \vec{e}_1)^2}{\omega_1^2(q)}, \quad (7)$$

where the sum over  $\vec{q}$  includes only those modes with wavelengths larger than the size of the system. The  $\omega_1$  and  $\vec{e}_1$  refer to the frequency and polarization of the longitudinal modes, respectively, and  $\Omega$  is the area of the macroscopic system. Evaluation of this sum in the long-wavelength limit gives an rms density fluctuation equal to  $0.014\rho_{\text{solid}}$  which is to be compared to a density difference of  $0.008\rho_{\text{solid}}$  from Fig. 7. This does not

prove rigorously that the two-phase region is unstable to density fluctuations. However, it does indicate that the long-wavelength fluctuations which are suppressed by the finite size of the system will tend to shift the balance in favor of the continuous transition and against the first-order transition. These large-amplitude density fluctuations are consistent with the view that the transition is continuous.

A proper treatment of the melting transition must include transverse modes (these generate the dislocations) and energy fluctuations. Such a treatment of the long-wavelength modes is beyond what we wish to do here. However, such considerations may be treatable in conjunction with a molecular-dynamics calculation in a manner similar to the Monte Carlo renormalization-group calculations that have been applied to spin systems.<sup>29</sup> Any pure simulation, be it molecular dynamics or Monte Carlo, will always be plagued by finite-sampling and finite-size constraints.

#### ACKNOWLEDGMENTS

This research was supported in part by the NSF under Grant No. DMR-8009251.

#### APPENDIX

The usual method of initializing a molecular-dynamics run is to place the particles in a perfect lattice and then to give each particle a random displacement relative to its lattice site and a random initial velocity.<sup>20</sup> Heating and cooling usually take place by the spontaneous increasing or decreasing of the kinetic energy of each particle. These procedures can produce configurations which are very far from equilibrium and may contain local configurations which are highly unlikely for a system near equilibrium. To avoid any such problems, a quasiharmonic nearest-neighbor lattice-dynamics<sup>30</sup> calculation was used to initialize the system. This determined both the initial displacement and the initial velocity for each particle. The amplitude of each harmonic wave was calculated using the standard classical formula relating temperature to amplitude and the phase of each wave was chosen at random. Once initial positions and velocities were determined, the *exact* equations of motion were integrated to allow the system to come to equilibrium. Although the lattice dynamics does not produce a state of equilibrium, it does produce

one with reasonable local configurations, that is, without any particle being very close to another or having a very large velocity. Furthermore, with some experience, it was quite possible to predict within a few percent what input "temperature" was required for the initialization to result in a desired final energy or temperature of the model system. Energy values for several runs were obtained by appropriate heating or cooling procedures. Furthermore, more than one initialization was used to avoid the possibility of being trapped in a narrow region of phase space. Many of these runs were used to check the data reported here but are not shown explicitly.

Heating or cooling was performed by applying to each particle a "viscous" force  $\vec{f}$  proportional to the particle's velocity  $v$  with

$$\vec{f} = b\vec{v}. \quad (\text{A1})$$

Then the exact equations of motion were integrated. For cooling one needs  $b < 0$ , while for heating,  $b > 0$ . While heating, it is necessary to correct the total momentum of the system at every time step because computer round-off error guarantees that the model system will always have some small total momentum. A positive  $b$  will always produce a net increase in any initial total momentum. Each heating or cooling cycle consisted of approximately 200 steps during which the "viscous" force was turned on and then 1000 steps at constant energy. This configuration was then used as the initial configuration of a constant-energy run. From a single initialization, several constant-energy runs were obtained by either heating or cooling the system by small amounts. For those runs obtained by *heating* some initial configuration, the heating process usually was started from a configuration which had been run at constant energy for about 1000 time steps. *However*, for the set of runs which were generated by cooling, the cooling process was started from a configuration which was run at constant energy for one relaxation time or for 50 000 time steps, whichever came first. This was done in an attempt to avoid changing the energy of the system before the effects of the last cooling process had damped out.

The value of the time interval used for each time step was determined by requiring energy conservation over the entire energy range of interest and over the longest run used. Near the transition, runs of nearly 100 000 time steps were typically used. A single time step was about  $0.02\tau$ , which means that runs were typically about  $1800\tau$  near

the transition. Energy conservation held to about four or five significant features. How much, if any, of a given run was included in the thermo-

dynamic average was determined by an examination of the time dependence of appropriate auto-correlation functions.

- 
- <sup>1</sup>J. P. McTague, D. Frankel, and M. P. Allen, in *Ordering in Two Dimensions*, edited by S. K. Sinha (North-Holland, New York, 1980), p. 147.
- <sup>2</sup>F. F. Abraham, in *Ordering in Two Dimensions*, Ref. 1, p. 155.
- <sup>3</sup>J. Tobochnik and C. V. Chester, in *Ordering in Two Dimensions*, Ref. 1, p. 339.
- <sup>4</sup>J. M. Kosterlitz and D. J. Thouless, *J. Phys. C* **6**, 1181 (1973).
- <sup>5</sup>B. I. Halperin and D. R. Nelson, *Phys. Rev. Lett.* **41**, 121 (1978).
- <sup>6</sup>D. R. Nelson and B. I. Halperin, *Phys. Rev. B* **19**, 2457 (1979).
- <sup>7</sup>A. P. Young, *Phys. Rev. B* **19**, 1855 (1979).
- <sup>8</sup>B. J. Alder and T. E. Wainwright, *Phys. Rev.* **127**, 359 (1962).
- <sup>9</sup>F. Tsien and J. P. Valleau, *Mol. Phys.* **27**, 177 (1974).
- <sup>10</sup>D. Frenkel and J. P. McTague, *Phys. Rev. Lett.* **42**, 1632 (1979).
- <sup>11</sup>R. H. Morf, *Phys. Rev. Lett.* **43**, 931 (1979).
- <sup>12</sup>R. K. Kalia, D. Varshishta, and S. D. de Leeuw, *Phys. Rev. B* **23**, 4794 (1981).
- <sup>13</sup>J. A. Barker, D. Henderson, and F. F. Abraham, *Physica* **106A**, 226 (1981).
- <sup>14</sup>F. van Swol, L. V. Woodcock, and J. N. Cape, *J. Chem. Phys.* **73**, 913 (1980).
- <sup>15</sup>S. Toxvaerd, *Phys. Rev. Lett.* **44**, 1002 (1980).
- <sup>16</sup>F. F. Abraham, *Phys. Rev. B* **23**, 6145 (1981).
- <sup>17</sup>J. Q. Broughton, G. H. Gilmer, and J. D. Weeks, *Phys. Rev. B* **25**, (1982).
- <sup>18</sup>J. D. Weeks, *Phys. Rev. B* **24**, 1530 (1981).
- <sup>19</sup>W. G. Hoover, S. G. Gray, and K. W. Johnson, *J. Chem. Phys.* **55**, 1128 (1971).
- <sup>20</sup>F. H. Ree, in *Physical Chemistry 8A*, edited by H. Eyring, D. Henderson, and W. Jost (Academic, New York, 1971), p. 157.
- <sup>21</sup>T. L. Hill, *Statistical Mechanics* (McGraw-Hill, New York, 1956), p. 422.
- <sup>22</sup>M. J. Mandell, J. P. McTague, and A. Rachman, *J. Chem. Phys.* **66**, 3070 (1977).
- <sup>23</sup>J. L. Lebowitz, J. K. Percus, and L. Varlet, *Phys. Rev.* **153**, 250 (1967).
- <sup>24</sup>P. A. Egelstaff, *Rep. Prog. Phys.* **29**, 333 (1966).
- <sup>25</sup>H. E. Stanley, G. Paul, S. Milosevic, in *Physical Chemistry 8B*, edited by H. Eyring, D. Henderson, and W. Jost (Academic, New York, 1971), p. 866.
- <sup>26</sup>P. Schofield, *Proc. Phys. Soc. London* **88**, 149 (1966).
- <sup>27</sup>W. M. Lomer and G. G. Low, in *Thermal Neutron Scattering*, edited by P. A. Egelstaff (Academic, New York, 1963), p. 28.
- <sup>28</sup>W. Nowacki, *Dynamics of Elastic Systems* (Wiley, New York, 1963), p. 279.
- <sup>29</sup>R. H. Swendsen, *Phys. Rev. Lett.* **42**, 859 (1979).
- <sup>30</sup>R. A. Cowley, *Rep. Prog. Phys.* **31**, 123 (1968).